

## Itinerant versus localized transport in $\text{La}_{1-x}\text{SrxMnO}_3$ for $x \lesssim 0.175$

Andrei Pimenov, Christine Hartinger, Alois Loidl, A. A. Mukhin, V. Yu. Ivanov, A. M. Balbashov

### Angaben zur Veröffentlichung / Publication details:

Pimenov, Andrei, Christine Hartinger, Alois Loidl, A. A. Mukhin, V. Yu. Ivanov, and A. M. Balbashov. 1999. "Itinerant versus localized transport in  $\text{La}_{1-x}\text{SrxMnO}_3$  for  $x \lesssim 0.175$ ." *Physical Review B* 59 (19): 12419–24. <https://doi.org/10.1103/PhysRevB.59.12419>.



## Itinerant versus localized transport in $\text{La}_{1-x}\text{Sr}_x\text{MnO}_3$ for $x \leq 0.175$

A. Pimenov, Ch. Hartinger, and A. Loidl  
*Institut für Physik, Universität Augsburg, 86135 Augsburg, Germany*

A. A. Mukhin and V. Yu. Ivanov  
*General Physics Institute, Russian Academy of Sciences, 105835 Moscow, Russia*

A. M. Balbashov  
*Moscow Power Engineering Institute, 105835 Moscow, Russia*  
(Received 16 November 1998)

The complex dielectric function  $\varepsilon_1 + i\varepsilon_2$  of  $\text{La}_{1-x}\text{Sr}_x\text{MnO}_3$  has been investigated for concentrations  $0.1 \leq x \leq 0.175$  near the metal-to-insulator transition. Quasioptical spectroscopy technique were employed for frequencies  $100 \text{ GHz} \leq \nu \leq 1100 \text{ GHz}$  and temperatures  $10 \text{ K} \leq T \leq 300 \text{ K}$ . Both, the dielectric constant  $\varepsilon_1$  and the conductivity  $\sigma_1 = \varepsilon_0 \varepsilon_2 \omega$  of all samples were found to increase on cooling through the magnetic-ordering transition. From this observation and from the analysis of the frequency dependencies we conclude that the charge carriers are localized in a broader range of the phase diagram than generally accepted. We show that hopping or tunneling between localized states dominates the conductivity for Sr concentrations  $x \leq 0.15$  and temperatures  $T < 300 \text{ K}$ . Even for  $\text{La}_{0.725}\text{Sr}_{0.175}\text{MnO}_3$  the localization effects are observed at least 10 K below the magnetic-phase transition. Finally, the dielectric constant is observed to diverge on approaching the metal-insulator transition. [S0163-1829(99)02519-9]

### I. INTRODUCTION

The observation of a negative colossal magnetoresistance<sup>1</sup> in the doped perovskite manganites has attracted much interest in these materials. The parent compound  $\text{LaMnO}_3$  is a semiconductor that orders antiferromagnetically below 140 K. The substitution of  $\text{La}^{3+}$  by a divalent alkaline-earth cation, such as  $\text{Sr}^{2+}$  or  $\text{Ca}^{2+}$ , induces mixed valency on the Mn side. The resulting composition can be represented in the form  $\text{La}_{1-x}^{3+}\text{A}_x^{2+}\text{Mn}_{1-x}^{3+}\text{Mn}_x^{4+}\text{O}_3$ . With increasing doping concentration  $x$  the conductivity of manganites increases, which can be attributed to the growing amount of holes in the lattice on  $\text{Mn}^{4+}$  sites. For  $x > 0.17$  the low-temperature resistivity shows a metallic character. The charge transfer in these compounds can be qualitatively understood using the double-exchange (DE) mechanism, which has been introduced by Zener.<sup>2</sup> Later on it has been realized that other effects (Jahn-Teller distortions, orbital order) play an important role in determining the conductivity and the magnetoresistance in the manganites.<sup>3</sup>

Within the framework of the double-exchange model, the ferromagnetic (FM) order at low temperatures favors the charge transfer between  $\text{Mn}^{3+}$  and  $\text{Mn}^{4+}$  ions and hence, strongly influences the hole mobility. As a result, the occurrence of magnetic order in the doped manganites is accompanied by a sharp decrease in resistivity at  $T = T_C$ , which has been interpreted as a semiconductor-metal transition. For further decreasing temperature, charge-ordering transition is observed at  $T = T_{CO}$  restoring the semiconducting behavior of the resistivity. It has been concluded that the doped manganites in this concentration range are metals between  $T_C$  and  $T_{CO}$ .<sup>4,5</sup> This conclusion is mainly based on the definition for metallic conduction as having the positive derivative  $d\rho/dT > 0$ . This concept, however, is hardly applicable in

the vicinity of phase transition, as the decrease on  $\rho(T)$  on decreasing temperature may be not due to the increase of metallicity but, for instance, caused by the decrease of the spin-disorder scattering at the magnetic-phase transition<sup>6</sup> or due to the strong increase of the hopping probability within the double-exchange model. Thus, the analysis of the temperature dependence of the dc resistivity alone do not allow the clear separation of metallic and the superconducting behavior. Strictly speaking, the clear definition of the metallic and the insulating state exists only for zero frequency and zero temperature.<sup>7,8</sup> At  $T \neq 0$  and  $\omega \neq 0$  the description quickly becomes more complicated. Therefore, for practical purposes we will not try to distinguish between the metallic and semiconducting state but mainly will be interested in the question “*Are the charge carriers in doped manganites localized or delocalized?*” and will focus on the regimes that reveal metalliclike behavior.

In the following we will try to find the answer to this question on the basis of the analysis of complex conductivity at finite frequencies and finite temperatures. As will be shown below, localized and delocalized states have completely different properties from the point of view of the frequency and temperature dependence of the complex conductivity.

In order to describe the frequency dependence in the delocalized state, the Drude model can be used:<sup>9,10</sup>

$$\sigma^*(\omega) = \sigma_1 + i\sigma_2 = \sigma_0(1 - i\omega\tau)^{-1}. \quad (1)$$

In this expression  $\sigma_0$  is the dc conductivity and  $\tau$  is the characteristic scattering rate. Equation (1) describes free charge carriers and it is important to note that the real part is nearly constant for  $\omega\tau \ll 1$  or a decreasing function of frequency  $d\sigma_1/d\omega < 0$ . Another characteristic feature of the

Drude process is a negative value of the real part of dielectric constant  $\epsilon_1 = -\sigma_2/\epsilon_0\omega < 0$ . The Drude model is applicable in the approximation of a single-collision frequency and well-defined elementary excitations. In a more general case, the damping term in the Drude equation is allowed to be complex and frequency dependent [ $\tau \rightarrow \tau^*(\omega)$ ].<sup>11,12</sup> The resulting expression, termed “modified Drude model” has been widely used recently to describe the complex conductivity of high- $T_C$  superconductors in the infrared frequency range.<sup>13</sup> However, the two mentioned features of the modified model except for exotic choice of  $\tau^*(\omega)$  remain the same:  $d\sigma_1/d\omega < 0$  and  $\epsilon_1 < 0$ .

On the contrary, using the mechanism of hopping or tunneling between the localized state one obtains the conductivity, which is an increasing function of frequency, and can be expressed by<sup>14</sup>

$$\sigma(\omega) = \sigma_0 + A\omega^s - iA\omega^s \tan(s\pi/2), \quad (2)$$

with the exponent  $s$ , which generally is lower than one. The frequency dependence of the dielectric constant [as extracted from Eq. (2)] is given by  $\epsilon_1 = A\omega^{s-1}\epsilon_0^{-1}\tan(s\pi/2)$  and is expected to hold only at high frequencies. In the low-frequency region ( $\omega < \omega_c$ ), where the dc term in the conductivity dominates, the complex conductivity takes the form<sup>15,16</sup>

$$\sigma(\omega)/\sigma(0) = 1 + i\alpha_1\varpi + \alpha_2\varpi^2, \quad \varpi = \omega/\omega_c, \quad (3)$$

and thus the dielectric constant levels off. In this equation  $\alpha_1$  and  $\alpha_2$  are constants and  $\omega_c$  is the characteristic frequency. Compared to Eq. (1), two main features of the hopping conductivity show completely opposite character: (i) the real part of conductivity is now an increasing function of frequency  $d\sigma_1/d\omega > 0$  and, (ii) the dielectric constant is positive,  $\epsilon_1 > 0$ .

Therefore, by measuring the frequency dispersion of the conductivity  $d\sigma_1(\omega)/d\omega$ , one obtains the tool to distinguish between localized and delocalized charge carriers at a given temperature, though it is not always easy to extract the electronic contribution from the spectra. Furthermore, the analysis of the sign of the dielectric constant  $\epsilon_1$  provides a second possibility to draw conclusions about the mechanism of the charge transfer.

In this paper we report on submillimeter-wave (100 – 1100 GHz) properties of  $\text{La}_{1-x}\text{Sr}_x\text{MnO}_3$  crystals of the concentration  $x = 0.125, 0.15,$  and  $0.175$ . We analyze the experimental data on the basis of the concepts presented above, in order to distinguish whether the complex conductivity shows localized or delocalized character.  $\text{La}_{0.875}\text{Sr}_{0.125}\text{MnO}_3$  and  $\text{La}_{0.85}\text{Sr}_{0.15}\text{MnO}_3$  were measured at temperatures between 10 and 300 K.  $\text{La}_{0.825}\text{Sr}_{0.175}\text{MnO}_3$  was measured between 270 and 300 K, i.e., above and few degrees below the ferromagnetic phase transition. Below 270 K the conductivity of  $\text{La}_{0.825}\text{Sr}_{0.175}\text{MnO}_3$  is too high to allow transmission measurement with our experimental setup. In addition, we include a discussion of the submillimeter properties of  $\text{La}_{0.9}\text{Sr}_{0.1}\text{MnO}_3$ , which were obtained by the same technique and were published previously.<sup>17</sup>

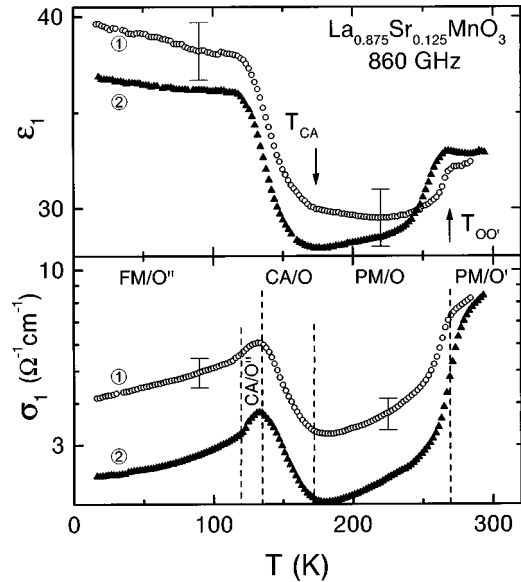


FIG. 1. Temperature dependence of the conductivity (lower panel) and the dielectric constant (upper panel) of  $\text{La}_{0.875}\text{Sr}_{0.125}\text{MnO}_3$  at  $\nu = 860$  GHz. Two curves represent two different optical axes of the sample. The phase-transition analysis is given according to Ref. 23. The notations are: PM — paramagnetic, CA — canted antiferromagnetic, FM — ferromagnetic, O — Jahn-Teller distorted orthorhombic phase, O' — nondistorted orthorhombic phase, O'' — the O' phase with an additional charge and orbital ordering, and R — rhombohedral phase.

## II. EXPERIMENT

Single crystals of  $\text{La}_{1-x}\text{Sr}_x\text{MnO}_3$  ( $x = 0.125, 0.15, 0.175$ ) were grown in the air by using a floating zone method with radiation heating.<sup>18</sup> X-ray powder diffraction measurements revealed that the grown materials were of single phase. Two-dimensional x-ray topography of the crystals indicated a twin structure of all crystals.

The temperature dependence of the dc resistivity<sup>19</sup> was measured using a four-point technique and resembles quantitatively and qualitatively the data known from literature.<sup>4,20</sup> Transmission experiments in the frequency range 100–1100 GHz were performed utilizing a set of backward-wave oscillators. The measurements were performed in a Mach-Zehnder interferometer arrangement,<sup>21</sup> which allows both the measurements of transmission and phase shift. Utilizing the Fresnel optical formulas, the conductivity and the dielectric constant were determined directly from the observed spectra without any approximations. The principal optical axis could be distinguished only for the  $x = 0.125$  sample, although the twinning did not allow the identification of specific directions. Due to the twinned structure of the samples investigated and because of possible phase-separation effects,<sup>22</sup> the measured conductivity spectra should be considered as averaged values across the sample.

## III. RESULTS AND DISCUSSION

Figure 1 shows the temperature dependence of the conductivity and the dielectric constant of  $\text{La}_{0.875}\text{Sr}_{0.125}\text{MnO}_3$ . Both functions reveal a complicated temperature dependence, which is a direct consequence of the complex phase

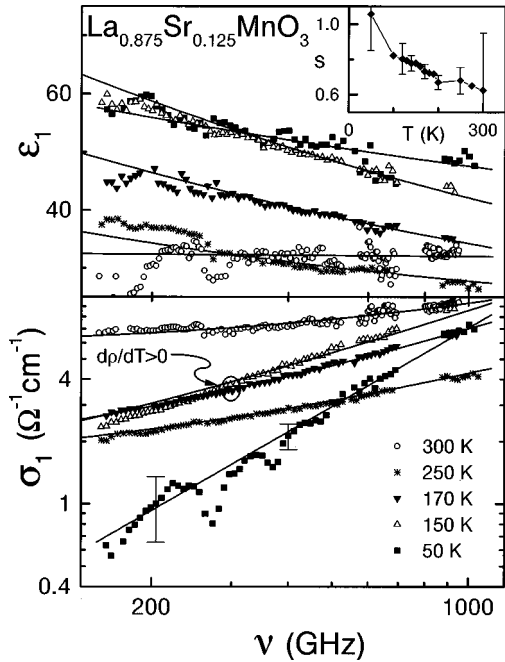


FIG. 2. Frequency dependence of the conductivity (lower panel) and the dielectric constant (upper panel) of  $\text{La}_{0.875}\text{Sr}_{0.125}\text{MnO}_3$  at different temperatures. The solid lines at  $T = 150\text{--}250$  K represent the fits according to Eq. (2). The lines at lowest and highest temperatures are guides to the eye. The inset shows the temperature dependence of the frequency exponent according to Eq. (2).

diagram of the Sr-doped manganites. In the following discussion of the observed anomalies of conductivity and dielectric constant we will use the notations of the recent paper of Paraskevopoulos *et al.*<sup>23</sup> They derived the magnetic-phase diagram on the basis of susceptibility and magnetization measurements of Sr-doped samples from the same batch. Though the low-temperature magnetic-phase diagram was critically reconsidered, the structural aspects remain similar to the known phase diagram.<sup>5,20</sup> According to the phase diagram,  $\text{La}_{0.875}\text{Sr}_{0.125}\text{MnO}_3$  is in a paramagnetic (P) state with an orthorhombic (O') structure at room temperature. A structural-phase transition to the Jahn-Teller distorted orthorhombic phase (O) takes place around  $T = 270$  K and clearly corresponds to a step of conductivity and the dielectric constant at 860 GHz in Fig. 1. On further decreasing temperature, the steep increase of  $\sigma_1(T)$  and  $\epsilon_1(T)$  is observed at  $T \approx 175$  K and coincide with the paramagnetic-to-canted-antiferromagnetic transition. Two further characteristic temperatures represent the transition into the charge-ordered O'' phase at  $T \approx 150$  K and the transition into the ferromagnetically ordered state  $T \approx 140$  K. Most probably the maximum of the dynamical conductivity at  $T \approx 130$  K and the small step in  $\sigma_1$  somewhat below this temperature correspond to these two transitions. A difference in the absolute values of the transition temperatures may be attributed to the slightly different oxygen stoichiometry of our samples. We note, that between  $T = 170$  and 130 K the dynamic (Fig. 1) and the dc conductivity (Ref. 19) both are decreasing functions of temperature, and thus possibly suggest the metallic and itinerant character of the charge-transfer mechanism.

Figure 2 shows the conductivity (lower panel) and the dielectric constant (upper panel) of  $\text{La}_{0.875}\text{Sr}_{0.125}\text{MnO}_3$  as a

function of frequency at different temperatures. The conductivity increases as a function of frequency at all temperatures investigated. This behavior is accompanied by a negative dispersion of the dielectric constant. Both effects agree well with the frequency dependence of hopping conductivity as given by Eq. (2). The temperature dependence of the effective frequency exponent  $s$  was extracted from the spectra using Eq. (2) and is presented in the inset of Fig. 2. The influence of the processes at higher frequencies was taken into account by adding a frequency independent  $\epsilon_\infty$  to the dielectric constant. The fits are represented as solid lines in Fig. 2. Due to the growing importance of phonon contributions at low temperatures the simultaneous fitting of conductivity and dielectric constant using Eq. (2) becomes poor for  $T < 130$  K. At these temperatures the absolute value of the frequency exponent was estimated solely from  $\sigma_1(\nu)$  data. The most interesting point is that even in the temperature range between 130 and 175 K the frequency dependence of complex conductivity remains nearly the same. Below  $T \approx 175$  K the sample becomes magnetically ordered and the change in slope from  $d\rho/dT < 0$  to  $d\rho/dT > 0$  is observed in both  $\sigma_{dc}(T)$  and  $\sigma_{ac}(T)$ . But also in this range the submillimeter spectra can well be described using Eq. (2), and this is a strong indication that hopping still dominates the charge transport. It is only the effective amplitude factor  $A$  of Eq. (2) that has a strong temperature dependence in the range between 130 and 175 K. Because of this dependence both the conductivity and the dielectric constant exhibit a simultaneous increase as the temperature is lowered below  $T_{CA} \approx 175$  K (Fig. 1). As mentioned in the introduction section, there is no need to suppose the itinerant character of electrons in this temperature range. Many other possible mechanisms, e.g., the freezing of the spin scattering or an increase of the hopping probability due to the magnetic ordering may explain the observed temperature dependence of resistivity without assuming the itinerant character of the charge-transfer process. Finally, we note that the observed behavior of the conductivity and the dielectric constant cannot be explained using the picture of delocalized carriers as given by Eq. (1) because the increase of the conductivity within this model would be followed by a decrease of dielectric constant, just the opposite to what is observed experimentally. Thus, we conclude that hopping between localized states remains the leading conductivity mechanism in  $\text{La}_{0.875}\text{Sr}_{0.125}\text{MnO}_3$  for all temperatures  $T < 300$  K.

Figure 3 shows the dielectric constant (upper panel) and the conductivity (lower panel) of  $\text{La}_{0.85}\text{Sr}_{0.15}\text{MnO}_3$  as a function of frequency. At low temperatures the conductivity is clearly an increasing function of frequency with a frequency exponent of about one. The apparent frequency dispersion of the conductivity becomes weaker with increasing temperature, which may be interpreted as a decrease of the effective frequency exponent. Because of the high value of dc conductivity, it is not possible to distinguish whether this temperature dependence of the frequency exponent represents the asymptotic high-frequency behavior ( $\omega^s$ ) or just is due to a crossover from  $\sigma_{dc}$  to  $\sigma_{ac}$ . Nevertheless, Fig. 3 indicates that hopping between localized carriers again is the dominating conductivity mechanism. This conclusion apparently contradicts the temperature dependence of the dc resistivity for temperatures just below  $T_C \approx 250$  K, where  $d\rho/dT > 0$ . In

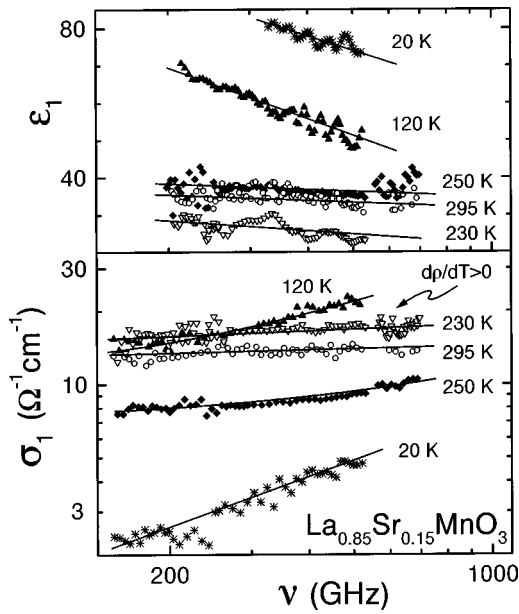


FIG. 3. Frequency dependence of the conductivity (lower panel) and the dielectric constant (upper panel) of  $\text{La}_{0.85}\text{Sr}_{0.15}\text{MnO}_3$  at different temperatures. The solid lines are guides to the eye.

order to further investigate this point, we turn to Fig. 4, which shows the temperature dependence of the conductivity and the dielectric constant of  $\text{La}_{0.85}\text{Sr}_{0.15}\text{MnO}_3$  at different frequencies. The behavior of the dielectric constant is more complicated than  $\epsilon_1(T)$  of  $\text{La}_{0.875}\text{Sr}_{0.125}\text{MnO}_3$  because the structural  $\text{OO}'$  transition almost coincides with the magnetic-ordering temperature. This transition is observed around 275 K for  $x=0.125$  (Fig. 1) and obviously causes the observed decrease of  $\epsilon_1(T)$  in  $\text{La}_{0.85}\text{Sr}_{0.15}\text{MnO}_3$ . The dielectric constant and the conductivity steeply increase as the sample is further cooled below  $T_C$ . This behavior again can

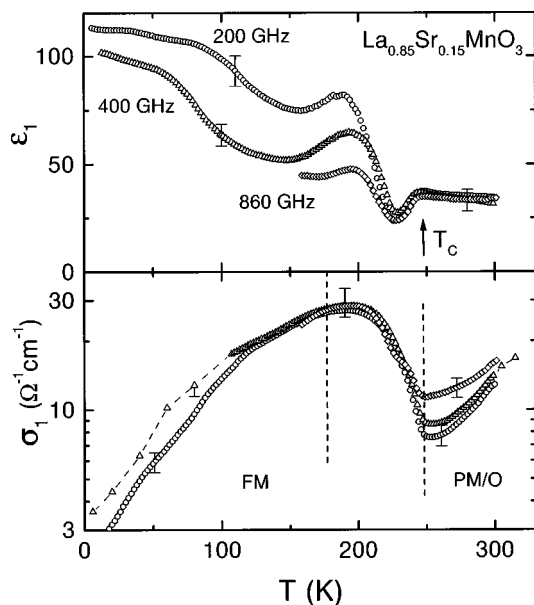


FIG. 4. Temperature dependence of the conductivity (lower panel) and the dielectric constant (upper panel) of  $\text{La}_{0.85}\text{Sr}_{0.15}\text{MnO}_3$  at different frequencies. The notations of different phases are the same as in Fig. 1.

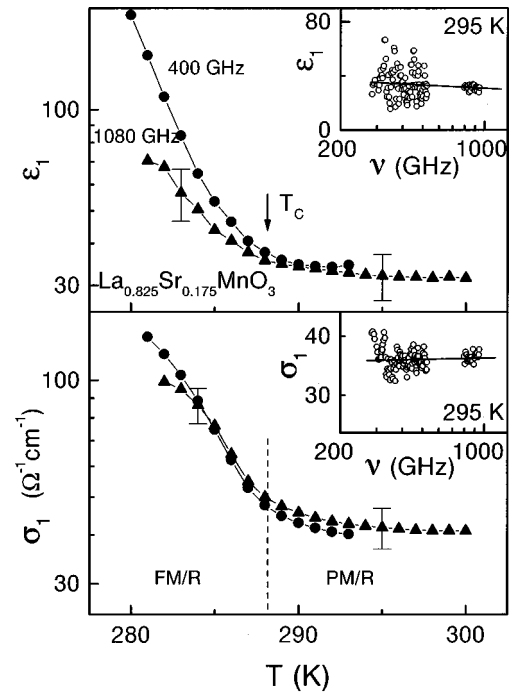


FIG. 5. Temperature dependence of the conductivity (lower panel) and the dielectric constant (upper panel) of  $\text{La}_{0.825}\text{Sr}_{0.175}\text{MnO}_3$  different frequencies. The notations of different phases are the same as in Fig. 1. The insets show the frequency dependence of  $\sigma_1$  (lower panel) and  $\epsilon_1$  (upper panel) at room temperature.

well be explained on the basis of Eq. (2), and thus confirms that hopping between localized carriers is the main mechanism of conductivity. An additional support of this conclusion is provided by the 230 K curve of Fig. 3. Even at this temperature, which lies in the middle of the “metallic” resistivity, the conductivity reveals a weak but definite positive-frequency dispersion.

The inset of Fig. 5 shows the frequency dependence of the conductivity and the dielectric constant of  $\text{La}_{0.825}\text{Sr}_{0.175}\text{MnO}_3$  at room temperature. Within the resolution of our spectrometer, both functions  $\epsilon_1(\nu)$  and  $\sigma_1(\nu)$  are frequency independent. At this point, two possible mechanisms can explain the observed behavior. As a first possibility, the conductivity may be due to the hopping process with the term  $\sigma_0$  Eq. (2) dominating the total contribution and, therefore, suppressing the dispersion of conductivity and dielectric constant. Second, the conductivity could be represented by the Drude model with the characteristic scattering rate much higher than the frequency range of present experiment  $\tau^{-1} \gg \nu$ . In this case also Eq. (1) yields a frequency-independent conductivity and dielectric constant. The observed positive value of the dielectric constant may be attributed to the phonon contribution at higher frequencies. In order to distinguish between these two possible explanations, we analyze the temperature dependence of the conductivity and the dielectric constant as presented in Fig. 5. As was already seen for  $\text{La}_{0.875}\text{Sr}_{0.125}\text{MnO}_3$  and  $\text{La}_{0.85}\text{Sr}_{0.15}\text{MnO}_3$ , both functions increase simultaneously as the sample is cooled below  $T_C=288$  K, and this behavior clearly excludes the Drude explanation of the conductivity mechanism. On the contrary, Eq. (2) with temperature-

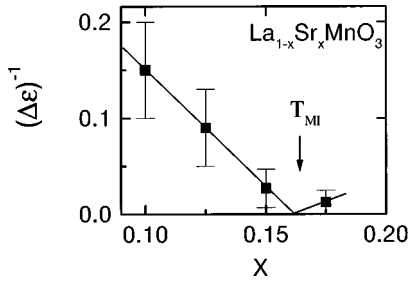


FIG. 6. Doping dependence of the absolute value of the dielectric constant step for  $\text{La}_{1-x}\text{Sr}_x\text{MnO}_3$ . The data for the Sr concentration  $x=0.1$  are taken from Ref. 17. The arrow marks the critical concentration of the metal-insulator transition.

dependent amplitude factor provides a natural explanation of the observed behavior. Thus, even in the apparently metallic region ( $d\rho/dT > 0$ ), the charge carriers still remain localized at least 10 K below the magnetic-ordering temperature.

The absolute value of the observed step of the dielectric constant continuously increases for increasing Sr doping. Although the specific values are frequency and orientation dependent, it is possible to estimate the approximate values in the submillimeter frequency region. In order to exclude the high-frequency phonon contribution to the dielectric constant, only the absolute values of the step of the dielectric function at the magnetic-ordering temperature will be analyzed. The phonon effects are assumed to be temperature independent. The values estimated in this way are:  $\Delta\varepsilon = 5 \div 10$  ( $x=0.1$ , Ref. 17);  $8 \div 20$  ( $x=0.125$ );  $25 \div 35$  ( $x=0.15$ ) and  $\Delta\varepsilon > 40 \div 90$  ( $x=0.175$ ) and are plotted inversely in Fig. 6 as a function of Sr doping. From Fig. 6 it is evident that  $\varepsilon_1$  diverges at a Sr concentration close to  $x=0.16$ , and thus resembles the well-known phenomena of dielectric catastrophe,<sup>24</sup> which has been observed in doped semiconductors in the vicinity the metal-insulator transition. On the basis of these data the Sr concentration of  $x=0.16$  can be identified as the critical concentration that determines the metal-insulator transition.

The remaining problem with  $\text{La}_{0.825}\text{Sr}_{0.175}\text{MnO}_3$  concerns the behavior of the complex conductivity at even lower temperatures than we were able to measure. At temperatures substantially lower than  $T_C$ , the magnetic moments are expected to be saturated and would not further influence the temperature dependence of conductivity. Thus, the metallic behavior of the resistivity ( $d\rho/dT > 0$ ) observed at low temperatures for  $\text{La}_{0.825}\text{Sr}_{0.175}\text{MnO}_3$ <sup>19,20</sup> seems to indicate the metallic character of conductivity in this range. Moreover, according to recent optical data,<sup>25</sup> a Drude-like peak is observed for  $\text{La}_{0.825}\text{Sr}_{0.175}\text{MnO}_3$  for  $T \lesssim 150$  K and the charge carriers seem to be delocalized at these temperatures. For  $T = 9$  K, the parameters of the Drude process were estimated to be  $\sigma_0 = 2600 \Omega^{-1} \text{cm}^{-1}$  and  $1/2\pi\tau = 16 \text{meV} = 3.9 \text{THz}$ . According to Eq. (1), these parameters correspond to a strong negative dielectric constant with the low-frequency limiting value of  $\varepsilon_1 = -1200$ . In order to retain agreement of all existing experimental data for  $\text{La}_{0.825}\text{Sr}_{0.175}\text{MnO}_3$ , we must suppose that the dielectric constant changes sign in the temperature range between 150 and 270 K. Furthermore, as the observed increase of  $\varepsilon_1$  indicates the approach of the insulator-to-metal transition, the change

of sign of  $\varepsilon_1$  has to be accompanied by a divergence of the dielectric constant. This effect should readily be observable in thin-film samples at submillimeter frequencies and will be investigated in a future paper.

Recently, studying the submillimeter properties of  $\text{La}_{1-x}\text{Sr}_x\text{MnO}_3$  single crystals with  $x=0.1$ , Ivanov *et al.*<sup>17</sup> have observed a jump of the dielectric constant around  $T = 100 - 120$  K. The authors have related this phenomenon to a polaron-ordering transition. Taking into account the above discussion and the experimental uncertainties, we can give an alternative explanation of the observed phenomena. The jump in the dielectric constant in  $\text{La}_{0.9}\text{Sr}_{0.1}\text{MnO}_3$  possibly results from the onset of magnetic order, and thus corresponds to the enhancement of the conductivity at  $T < T_{CA}$ . Similar to the samples with Sr concentrations  $0.125 \leq x \leq 0.175$ , this behavior is well explained by hopping or tunneling between localized states, described by Eq. (2) with the temperature-dependent amplitude parameter  $A$ .

On the basis of the above results we can give the following interpretation of the observed temperature dependencies of the conductivity and dielectric constant of the samples with Sr concentrations  $0.1 \leq x \leq 0.175$ . In the paramagnetic state, all the charge carriers are localized and the charge transfer takes place through the hopping or tunneling between localized states. Below  $T_{CA}$  the magnetic moments become increasingly ordered. This ordering strongly influences the hopping probability through the freezing of the spin scattering or, within the DE model, through an enhancement of the transfer probability between neighboring states. Although the exact microscopic mechanism of this influence is not well known up to now, the localized character of the conductivity is nevertheless retained. In agreement with Eq. (2), the simultaneous increase of conductivity and the dielectric constant can be phenomenologically described using the temperature-dependent amplitude parameter. In the doping range  $x \leq 0.15$ , even the full ordering of the magnetic moments is not sufficient to make the states delocalized. Few degrees below  $T_C$ , the magnetic moments are nearly fully ordered. As a result, the high-temperature activated behavior of the conductivity is recovered, but on the other quantitative level. Moreover, fine inspection of the temperature-dependent resistivity data of a high-quality  $\text{La}_{0.875}\text{Sr}_{0.125}\text{MnO}_3$  sample of Uhlenbruck *et al.*<sup>26</sup> in the temperature range between  $T_C$  and  $T_{CO}$  shows that the activated temperature dependence is recovered *before* the charge ordering takes place. It is therefore possible that the charge ordering observed for Sr concentrations  $0.1 \leq x \leq 0.15$  is not the absolute necessary condition to regain the activated behavior.

#### IV. CONCLUSIONS

Finally, we have investigated frequency and temperature dependence of the complex conductivity of  $\text{La}_{1-x}\text{Sr}_x\text{MnO}_3$  for Sr concentrations  $0.1 \leq x \leq 0.175$ . As temperature is lowered through the magnetic-phase transition point, all samples show a simultaneous increase of the conductivity and the dielectric constant. Based on this observation and on positive frequency dispersion of  $\sigma_1(\nu)$  of  $\text{La}_{0.875}\text{Sr}_{0.125}\text{MnO}_3$  and  $\text{La}_{0.85}\text{Sr}_{0.15}\text{MnO}_3$ , we conclude that the hopping or tunneling

between localized states remains the leading conductivity mechanism in the whole temperature range. Surprisingly,  $\text{La}_{0.825}\text{Sr}_{0.175}\text{MnO}_3$  also shows hopping behavior even 10 K below the magnetic-phase transition, where the conductivity

is expected to be metallic according to dc-resistivity data. Finally, the absolute value of the dielectric constant for Sr concentrations  $0.1 \leq x \leq 0.175$  shows the tendency to diverge on approaching a critical Sr concentration.

- <sup>1</sup>K. Chahara, T. Ohno, M. Kasai, and Y. Kozono, *Appl. Phys. Lett.* **63**, 1990 (1993); R. von Helmolt, J. Wecker, B. Holzapfel, L. Schultz, and K. Samwer, *Phys. Rev. Lett.* **71**, 2331 (1993); S. Jin, T. H. Tiefel, M. McCormack, R. A. Fastnacht, R. Ramesh, and L. H. Chen, *Science* **264**, 413 (1994).
- <sup>2</sup>C. Zener, *Phys. Rev.* **82**, 403 (1951).
- <sup>3</sup>A. J. Millis, P. B. Littlewood, and B. I. Shraiman, *Phys. Rev. Lett.* **74**, 5144 (1995); I. Solovyev, N. Hamada, and K. Terakura, *ibid.* **76**, 4825 (1996).
- <sup>4</sup>Y. Moritomo, A. Asamitsu, and Y. Tokura, *Phys. Rev. B* **56**, 12 190 (1997).
- <sup>5</sup>H. Kawano, R. Kajimoto, M. Kubota, and H. Yoshizawa, *Phys. Rev. B* **53**, 14 709 (1996).
- <sup>6</sup>C. M. Varma, *Phys. Rev. B* **54**, 7328 (1996).
- <sup>7</sup>N. F. Mott, *Metal-Insulator Transitions* (Taylor & Francis, London, 1990), p. 19.
- <sup>8</sup>F. Gebhard, *The Mott Metal-Insulator Transition* (Springer, Berlin, 1997).
- <sup>9</sup>P. Y. Yu and M. Cardona, *Fundamentals of Semiconductors* (Springer, Berlin, 1996), p. 296.
- <sup>10</sup>N. F. Mott and E. A. Davis, *Electronic Processes in Non-Crystalline Materials* (Oxford Press, Oxford, 1979), p. 15.
- <sup>11</sup>W. Götze and P. Wölfle, *Phys. Rev. B* **6**, 1226 (1972).
- <sup>12</sup>J. W. Allen and J. C. Mikkelsen, *Phys. Rev. B* **15**, 2952 (1977).
- <sup>13</sup>D. B. Tanner and T. Timusk, in *Physical Properties of High Temperature Superconductors III*, edited by D. M. Ginsberg (World Scientific, Singapore, 1992), p. 363.
- <sup>14</sup>A. K. Jonscher, *Nature* (London) **267**, 673 (1977); *Dielectric Relaxation in Solids* (Chelsea Dielectrics, London, 1983).
- <sup>15</sup>A. R. Long, *Hopping Transport in Solids* (Elsevier, Amsterdam, 1991).
- <sup>16</sup>H. Böttger and V. V. Bryksin, *Hopping Conduction in Solids* (Academie-Verlag, Berlin, 1985), p. 213.
- <sup>17</sup>V. Yu. Ivanov, V. D. Travkin, A. A. Mukhin, S. P. Lebedev, A. A. Volkov, A. Pimenov, A. Loidl, A. M. Balbashov, and A. V. Mozhaev, *J. Appl. Phys.* **83**, 7180 (1998); A. A. Mukhin, V. D. Travkin, V. Yu. Ivanov, S. P. Lebedev, A. A. Volkov, A. M. Balbashov, A. V. Mozhaev, A. M. Kadomtseva, Yu. F. Popov, and G. P. Vorob'ev, *J. Magn. Magn. Mater.* **183**, 160 (1998).
- <sup>18</sup>A. M. Balbashov, S. G. Karabashev, Ya. M. Mukovskii, and S. A. Zverkov, *J. Cryst. Growth* **167**, 365 (1996).
- <sup>19</sup>A. A. Mukhin, V. Yu. Ivanov, V. D. Travkin, S. P. Lebedev, A. Pimenov, A. Loidl, and A. M. Balbashov, *Pis'ma Zh. Eksp. Teor. Fiz.* **68**, 33 (1998) [*JETP Lett.* **68**, 356 (1998)].
- <sup>20</sup>A. Urushibara, Y. Moritomo, T. Arima, A. Asamitsu, G. Kido, and Y. Tokura, *Phys. Rev. B* **51**, 14 103 (1995).
- <sup>21</sup>A. A. Volkov, Yu. G. Goncharov, G. V. Kozlov, S. P. Lebedev, and A. M. Prochorov, *Infrared Phys.* **25**, 369 (1985).
- <sup>22</sup>E. L. Nagaev, *Phys. Usp.* **39**, 781 (1996); G. Allodi, R. De Renzi, G. Guidi, F. Licci, and M. W. Pieper, *Phys. Rev. B* **56**, 6036 (1997); S. Yunoki, J. Hu, A. L. Malvezzi, A. Moreo, N. Furukawa, and E. Dagotto, *Phys. Rev. Lett.* **80**, 845 (1998).
- <sup>23</sup>M. Paraskevopoulos, J. Hemberger, A. Loidl, A. A. Mukhin, V. Yu. Ivanov, and A. M. Balbashov, cond-mat/9812276 (unpublished).
- <sup>24</sup>N. F. Mott, *Metal-Insulator Transitions* (Ref. 7), p. 157.
- <sup>25</sup>Y. Okimoto, T. Katsufuji, T. Ishikawa, T. Arima, and Y. Tokura, *Phys. Rev. B* **55**, 4206 (1997).
- <sup>26</sup>S. Uhlenbruck, R. Teipen, R. Klingeler, B. Büchner, O. Friedt, M. Hücker, H. Kierspel, T. Niemöller, L. Pinsard, A. Revcolevschi, and R. Gross, *Phys. Rev. Lett.* **82**, 185 (1999).